

Image-Based Modelling of Soft Tissue Deformation

Mohamed A. ElHelw, Adrian J. Chung, Ara Darzi, and Guang-Zhong Yang

Royal Society/Wolfson Medical Image Computing Laboratory,
Imperial College London, London, United Kingdom
{mohammed.elhelw, ajchung, a.darzi, g.z.yang}@imperial.ac.uk

Abstract. This paper describes a novel method for simulating soft tissue deformation with image-based rendering. It is based on the association of a depth map with the texture image and the incorporation of micro-surface details to generate photorealistic images representing soft tissue deformations. In a pre-processing step, the depth map describing the surface is separated into two distributions corresponding to macro- and micro-surface details. During user interactive simulation, deformations resulting from tissue-instrument interaction are rapidly calculated by modifying a coarse mass-spring model fitted to the macro-surface structure. Micro-surface details are subsequently augmented to the modified model with 3D image warping. The proposed technique drastically reduces the polygonal count required to model the scene whilst preserving deformed small surface details to offer a high level of photorealism.

1 Introduction

Over the last ten years there has been a strong movement towards improved techniques of minimal access surgery. Endoscopy, including bronchoscopy and laparoscopy, is the most common procedure in minimal access surgery, which is carried out through natural body openings or small artificial incisions. If handled properly, endoscopes are completely harmless to patients. Diagnostic endoscopy can achieve its clinical goals with minimal inconvenience to patients. Compared with conventional techniques, patient trauma and hospitalisation can be greatly reduced and diagnostic accuracy and therapeutic success increased. However, the complexity of instrument controls, restricted vision and mobility, difficult hand-eye co-ordination and the lack of tactile perception require a high degree of manual dexterity of the operator. Consequently much attention has been paid to new training methods for these skills. Computer simulation provides an attractive possibility for certain aspects of this training, particularly for hand eye co-ordination. The benefits of endoscopic training through computer simulation, rather than the traditionally performed one-to-one apprenticeship schemes, are now well accepted in the medical community. It has been proven to be an economical and time saving solution for acquiring, as well as assessing basic surgical skills.

Hitherto, a significant amount of research has been carried out in the area of minimal access surgical simulators. One of the major challenges of these systems is the creation of photo-realistic rendering. Due to the complexity of geometry used to represent internal body organs and the fact that they are all non-rigid, the realism of de-

formations is a key research focus in surgical simulation [6]. In this paper we present a novel technique for soft tissue modelling which offers both visual realism and interactive tissue deformations. This is accomplished by combining the promise of photorealism offered by image-based rendering with the efficiency of mass-spring tissue deformation modelling.

1.1 Image-Based Rendering

Image-based rendering (IBR) has established itself as a powerful alternative to conventional geometry-based computer graphics. A set of images or depth-enhanced images is used to synthesise novel views of either synthetic or real environments. Texture mapping [5] is one of the earliest IBR methods used to represent complex materials that are hard to model and render. A major limitation of texture mapping is that texture mapped surfaces still appear as flat polygons onto which 2-D images are projected. They lack 3D details and do not exhibit appropriate parallax as the view-point changes. To address these problems, several extensions had been proposed in the past. Blinn [2] developed a bump mapping technique that enables the surface to appear dimpled by applying perturbations to its normals. The results, however, are not always convincing especially when viewed from certain positions, as silhouette edges can appear to pass through depressions [13]. Other methods such as height fields and displacement maps have proven to be either difficult to calculate or computationally prohibitive.

Better illusion of depth can be achieved at interactive frame rates by using image-based rendering methods where a depth map is used along with the texture image in the rendering process. The depth map models the details of the surface to be textured. This is referred to as image-based rendering by warping (IBRW) [12]. At run-time, the depth information at each image point is projected onto the viewing manifold to achieve photo-realistic rendering.

1.2 Soft Tissue Modelling

Deformable tissues can be geometrically represented as a set of surfaces or volumes. The choice of representation is dependent on two factors: computational efficiency and physical accuracy [7]. Surface models are faster to render since the number of vertices used to represent the surface are fewer than those used in the volumetric approach, though simulated deformations are less accurate.

Several methods for modelling soft tissue deformation have been introduced. They can be divided into three main categories: non-physical models, finite element models and mass-spring models. Non-physical models are parameter-based representations that include splines, patches, and free-form deformations. The curve or surface is defined using a set of control points. Although these methods are sufficient for some simulations, they are not widely used in medical simulations because of the difficulty in computing the parameters required to accurately deform the model. Finite element models, on the other hand, provide accurate deformations. The deformable surface is described as a collection of basic elements such as triangles and quadrilaterals where shape functions are defined [7]. This leads to the surface being treated as a continuum model with deformation equations derived from continuum mechanics [8].

Although much research has been carried out in using finite element methods in real-time tissue deformations [3,4], their general applications were limited by their extensive computational requirements, especially when the surface exhibits large shape changes. Real-time tissue deformations are usually achieved by using mass-spring models where the object is modelled as a collection of masses connected by springs. Mass-spring models only represent an approximation to real-world physics however, they are characterized by their relative ease of implementation and well-understood dynamics [14]. In the work presented, we integrate 3D image warping with mass-spring tissue modelling to achieve realistic simulations; *i.e.* real-time deformation behavior and visual realism. Implementation details and issues related to 3D perspective accuracy are discussed.

2 Method

The proposed method uses colour and depth information to simulate tissue deformation. While the colour image captures the photometric properties of the surface, the depth image describes the orthogonal distance from each image point to the modelled surface. Therefore, the depth image is considered as a modelling primitive that implicitly describes detailed surface geometry. In a pre-processing step, filtering is used to separate the depth image into macro- and micro-surface structures. The micro-structure represents important surface details, which are difficult to be modelled by soft tissue deformation, whereas the macro-structure is the one derived from interactive tissue deformation. In this framework, a coarse mass-spring model can be fitted to the macro-structure model, thus allowing rapid computation of interactive deformation. The use of IBR enables the augmentation of microscopic surface details, permitting photorealistic rendering of soft tissue undergoing deformation.

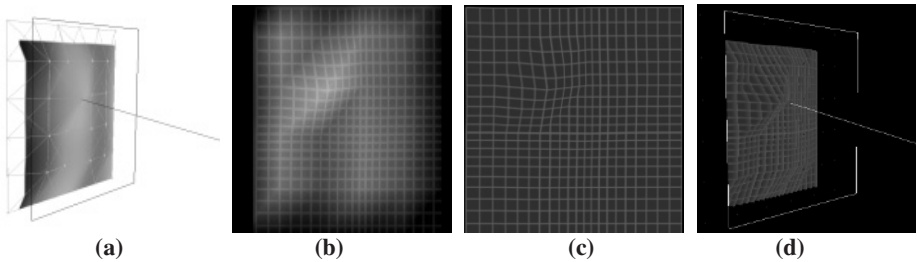


Fig. 1. Deformation when the surface is pulled outwards, where (a) illustrates a mass-spring model fitted to the macro-surface structure and (b) shows the combined deformed macro- and micro-surface structures. Images (c) and (d) are the distorted texture image and its 3D rendering respectively.

The process of simulating tissue deformation is illustrated in Figure 1. The macro-structure is efficiently deformed by using a low-resolution mass-spring model; subsequently micro-structure information is added. The texture image is distorted to conform to the deformed surface structures. Image-based rendering is used afterwards to render the deformed surface.

2.1 Mass-Spring-Damper Model

Simulating tissue deformations using a mass-spring-damper model is a well-established technique. A mass is assigned to each vertex in the geometric model describing the surface, then the masses are connected using springs and dampers. When a force acts upon the surface, the movement of a single mass point is computed using Newton's second law of motion. In a dynamic system, the motion of the point is given as

$$m_i a_i = -\mu v_i + \sum_j x_{ij} + f_i \quad (1)$$

where a_i is the resultant acceleration of point i with mass m_i due to forces applied by neighbouring springs, $\sum_j x_{ij}$, and other external forces, f_i , such as user and gravity

forces. The term $-\mu v_i$ is used to ensure system stability where μ_i is a damping coefficient and v_i is the speed of point i . As the system progresses through time, the point's new position is calculated by solving the differential equation.

Since the described image-based solution separates deformation modelling from rendering, different deformable models can be used, such as finite element methods with hierarchical mesh refinement, where more accurate deformations are required.

2.2 3D Image Warping

By using the plenoptic function approximation [1], which describes everything visible from a given point in space, we define the mappings from one image to another as image warps [9]. 3D image warping is a geometric operation where visible reference image points with depth are mapped onto a target image. Along with the reference camera model, the depth information provides a representation of the structure of the scene. A 3D point X seen through two different image planes, the reference and target cameras image planes, with centres of projection C_1 and C_2 respectively (Figure 2a), can be defined as:

$$X = C_1 + t_1 M_1 \bar{x}_1 = C_2 + t_2 M_2 \bar{x}_2 \quad (2)$$

where M_1 and M_2 describe the reference and target camera models, $x_1=(u_1, v_1)$ and $x_2=(u_2, v_2)$ are reference and target camera image plane points and t_1 and t_2 are reference and target camera constant scaling factors, all respectively. By expanding and rearranging terms of equation 2, the following 3D image warping equation can be derived [9],

$$\bar{x}_2 = \delta(x_1) M_2^{-1} (C_1 - C_2) + M_2^{-1} M_1 \bar{x}_1 \quad (3)$$

where $\delta(x_1)$ is the depth at reference image point x_1 . Therefore, a new image can be rendered from a nearby target viewpoint by projecting the reference image pixels to their 3D positions then re-projecting them onto the target image plane.

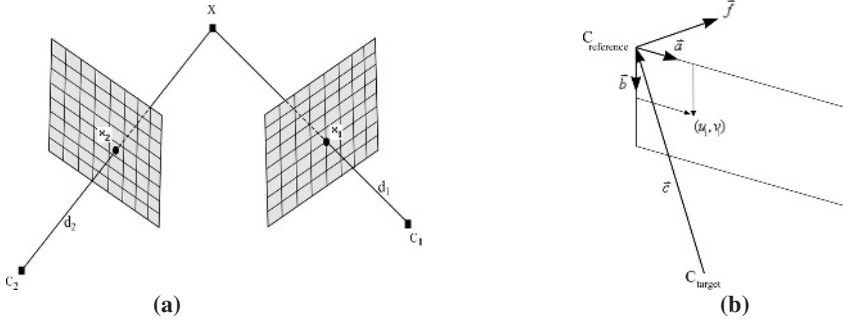


Fig. 2. (a) A 3D point X can be defined by using the camera centre-of projection C_i , image plane point x_i and scalar value t_i along the ray d_i from C_i through x_i for both reference and target cameras, where $i=1$ and 2 respectively (b) If the reference and target camera image planes coincide, 3D image warping equation simplifies to relief texture mapping equations.

By assuming a parallel-projection reference camera model and making both reference and target image planes coincide, as illustrated in Figure 2b, the 3D image warping equation simplifies to the relief texture mapping equations [10],

$$u_2 = \frac{\bar{a} \cdot (\bar{b} \times \bar{c}) u_1 + \bar{f} \cdot (\bar{b} \times \bar{c}) \text{displ}(u_1, v_1)}{\bar{c} \cdot (\bar{a} \times \bar{b}) + \bar{f} \cdot (\bar{a} \times \bar{b}) \text{displ}(u_1, v_1)} \quad (4)$$

$$v_2 = \frac{\bar{b} \cdot (\bar{c} \times \bar{a}) v_1 + \bar{f} \cdot (\bar{c} \times \bar{a}) \text{displ}(u_1, v_1)}{\bar{c} \cdot (\bar{a} \times \bar{b}) + \bar{f} \cdot (\bar{a} \times \bar{b}) \text{displ}(u_1, v_1)} \quad (5)$$

where \bar{a} and \bar{b} are the reference image plane basis vectors in Euclidean space, \bar{c} is the vector from target camera centre-of-projection to the origin of the reference image plane, \bar{f} is the vector perpendicular to the reference image plane, $\text{displ}(u, v_1)$ is the depth at reference image plane point (u, v_1) , and (u_2, v_2) is the target image plane point.

Relief texturing is used in the presented image-based approach to render the deformed surface. The process is carried out in two steps [11]: first, an intermediate image is generated by warping the source image to a plane that has exactly the same position, dimensions, and orientation as the destination polygon, then the intermediate image is texture-mapped onto the destination polygon using texture mapping hardware.

3 Results

To demonstrate the visual realism achieved by using the described technique, two experiments have been implemented to simulate deformable human tissues. The first system employs conventional geometry-based tissue deformation with a mass-spring model, while the second uses the image-based approach. Views from both systems are shown in Figure 3, from which it is evident that the image-based method provides

enhanced visual realism and better image quality over the conventional method. It can be noticed that when the tissue is deformed, the 3D structure of micro-surface elements is still preserved, resulting in rich surface details (Figure 3 left column). This becomes noticeable when the surface is viewed at sharp angles or from near view-points. Moreover, the texture pixelisation problem is minimised because the texture image is dynamically generated for each frame by means of 3D image warping.

The accuracy of the image-based technique is established through error analysis by comparing it to the polygon-based method used in conventional simulations.

Table 1. Error analysis for comparing the relative performance of image-based and polygon-based methods at different viewing angles

Incident Viewing Angle (degrees)	Mean Projection Error in Pixels	
	Image-Based Method	Polygon Method
11	10.140	10.104
14	10.013	11.548
19	8.5482	15.511
21	8.3895	15.317
23	8.2596	16.261

In Table 1, error is defined as the screen-space distance in pixels between the projections of selected texels and the projections of the corresponding object-space points. The scale of pixels in the rendered images is illustrated in Figure 3 (a4). From Table 1, it can be seen that the overall mean error is decreased by using the image-based technique. It can also be observed that unlike the image-based method, increasing the viewing angle results in increasing the error for the polygon-based method.

4 Discussion and Conclusions

In this paper we have introduced a new image-based tissue deformation technique. It is shown that the separation of surface details into macro- and micro-structures allows for fast deformation calculations and photo-realistic rendering. By comparing the quality of the rendering results, it has been demonstrated that the described method offers significantly improved visual realism over conventional polygonal methods. The validity of the image-based technique has been established by simulated tissue deformations and quantitative error analysis. An area for future work is to extend the image-based method for more than one planar surface. Additional work can be also carried out in investigating the use of image-based lighting methods to further improve the realism of the rendered scene.

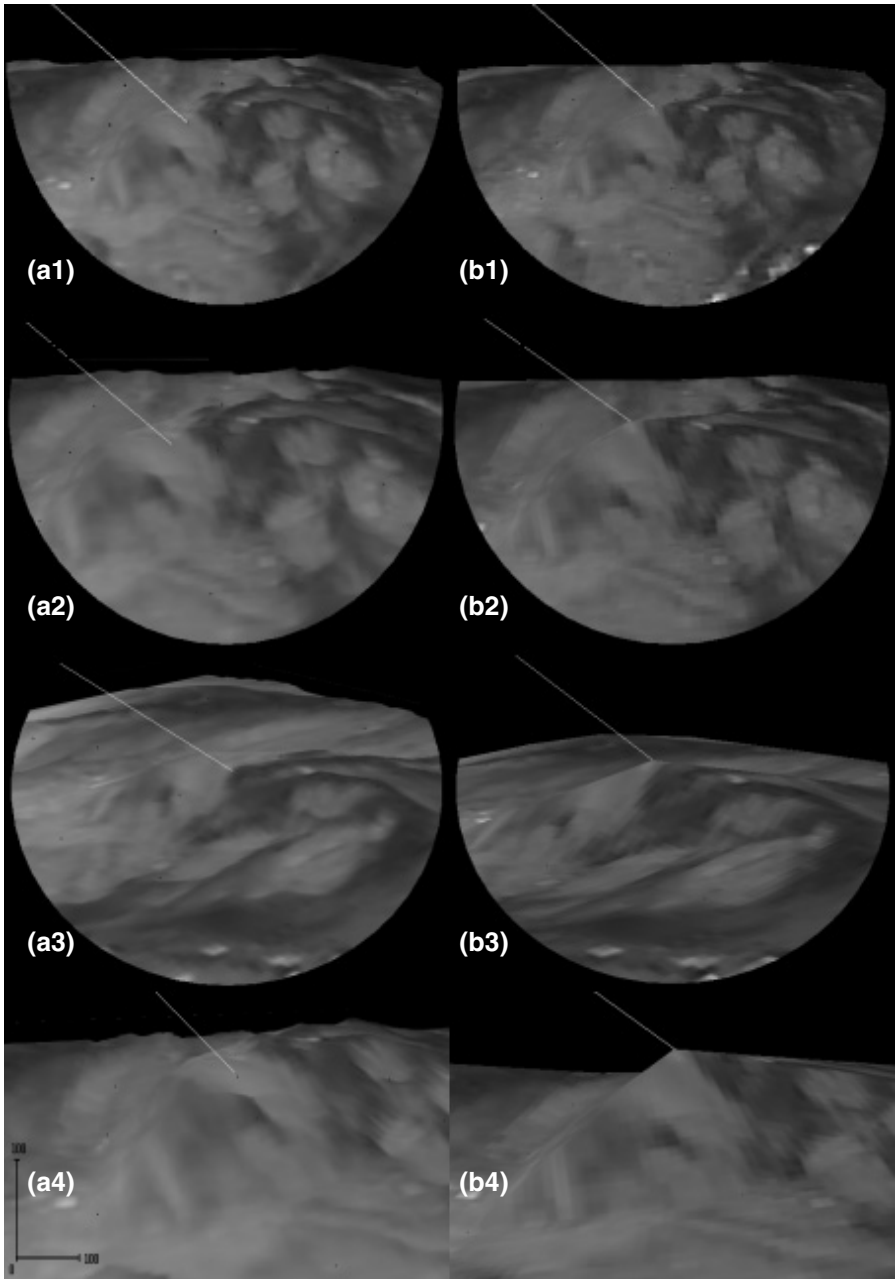


Fig. 3. Results from two deformable tissue simulations, where images on the left column (a1 to a4) are obtained by using the proposed image-based technique, and images on the right column (b1 to b4) are generated by using the conventional polygonal method.

References

1. Adelson E.H. and Bergen J.R. The Plenoptic Function and the Elements of Early Vision. Computational Models of Visual Processing, Chapter 1, Edited by Michael Landy and J. Anthony Movshon, The MIT Press, Cambridge, Massachusetts, 1991.
2. Blinn J. Simulation of Wrinkled Surfaces. Proceedings of Siggraph 1978, 286–292, 1978.
3. Bro-Nielsen, M. Fast Finite Elements for Surgery Simulation. Proceedings of Medicine Meets Virtual Reality 5 (MMVR '97), 395–400, 1997.
4. Bro-Nielsen M. and Cotin S. Real-time Volumetric Deformable Models for Surgical Simulation using Finite Elements and Condensation. Proceedings of Eurographics 1996, 57–66, 1996.
5. Catmull E. A Subdivision Algorithm for Computer Display of Curved Surfaces. Ph.D. Thesis, Department of Computer Science, University of Utah, Tech. Report UTEC-CSc-74–133, 1974.
6. Cotin S., Delingette H. and Ayache N. Real-time Elastic Deformations of Soft Tissues for Surgery Simulation. IEEE Transactions on Visualization and Computer Graphics, 5(1), 62–73, January-March 1999.
7. Delingette H. Towards Realistic Soft Tissue Modelling in Medical Simulation. INRIA. Report No 3506, September 1998. <http://www.inria.fr/Equipes/EPIDAURE-eng.html>
8. Gibson S.F.F. and Mirtich B. A Survey of Deformable Modelling in Computer Graphics. Mitsubishi Electric Research Laboratory – MERL. TR-97-19, November 1997.
9. McMillan L. An Image-Based Approach to Three-Dimensional Computer Graphics. Ph.D. Dissertation, UNC Computer Science Technical Report TR97-013, April 1997.
10. Oliveira M. Relief Texture Mapping. Ph.D. Dissertation, UNC CS Dept., Technical Report TR00-009, University of North Carolina, 2000.
11. Oliveira M., Bishop G., and McAllister D. Relief Texture Mapping. Proceedings of Siggraph 2000, 231–242, 2000.
12. Popescu V. Forward Rasterization: A Reconstruction Algorithm for Images-Based Rendering. Ph.D. Dissertation, UNC CS Dept., Technical Report TR01-019, University of North Carolina, 2001.
13. Watt A. 3D Computer Graphics. 3rd Edition, Addison Wesley, 2000.
14. Webster R, et al. Elastically Deformable 3D Organs for Haptic Surgical Simulation. Proceedings of Medicine Meets Virtual Reality (MMVR 02/10), 570–572, 2002.